Asian Journal of Chemistry; Vol. 26, No. 20 (2014), 6769-6779

ASIAN JOURNAL OF CHEMISTRY

http://dx.doi.org/10.14233/ajchem.2014.16741

Experimental Study of Vapor-Liquid Equilibrium and Optimization of Pressure-Swing Distillation for Methanol-Dimethyl Carbonate Binary System

JAESUK CHO[1], YU MI KIM[2], JAEHYUN NOH[3], DONG SUN KIM[1] and JUNGHO CHO[1,*]

[1]Department of Chemical Engineering, Kongju National University, Cheonan, Republic of Korea
[2]Process Solution Team, Kumho Petrochemical R&BD Center, Daejeon, Republic of Korea
[3]Department of Chemical Engineering, Hoseo University, Asan, Republic of Korea

*Corresponding author: Fax: +82 41 5542640; Tel: +82 41 5219366; E-mail: jhcho@kongju.ac.kr

Received: 22 November 2013; *Accepted*: 24 March 2014; *Published online*: 25 September 2014; AJC-16007

The mixture of methanol and dimethyl carbonate is characterized by an azeotropic point, thus, it is impossible to separate the azeotrope into respective high-purity products by general distillation. Herein, the separation of a methanol-dimethyl carbonate mixture *via* pressure-swing distillation was evaluated based on modeling and optimization of the separation process to obtain high-purity dimethyl carbonate. Currently, no experimental data on vapor-liquid equilibrium of methanol-dimethyl carbonate system is available in existing references. And even PRO/II, Aspen Plus, and ChemCAD simulation programs do not include a built-in binary interaction parameter of thermodynamic model of methanol-dimethyl carbonate system for accurate calculation. Therefore, the vapor-liquid equilibrium of the methanol-dimethyl carbonate binary system was experimentally evaluated under low-pressure and atmospheric pressure conditions and the binary interaction parameters were deduced from the non-random two-liquid model regression using the experimental data. The obtained binary interaction parameters were applied in modeling of the pressure-swing distillation process. Reboiler heat duty values from simulations under high-low pressure and low-high pressure configuration processes were compared and the process was optimized to minimize the heat duty.

Keywords: Dimethyl Carbonate, Vapor-liquid equilibrium, Pressure-swing distillation.

INTRODUCTION

Polycarbonates (PCs) are used in many fields, for electrical devices, electronic devices, vehicles, construction materials and optical materials owing to their promising properties such as heat resistance, impact resistance, dimensional stability and self-extinguishability[1]. Dimethyl carbonate (DMC), an intermediate material of PCs, is synthesized by the transesterification of ethylene carbonate (EC) with methanol as shown in Fig. 1[2]. Unreacted methanol and dimethyl carbonate are simultaneously obtained at the top of the distillation column; therefore, it is necessary to separate the two components to produce dimethyl carbonate with high-purity.

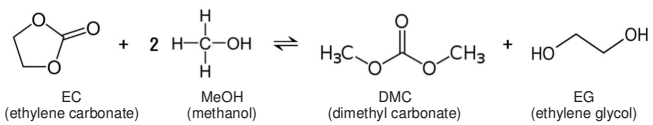

Fig. 1. Synthesis of dimethyl carbonate (DMC) by transesterification

The boiling point of dimethyl carbonate is 363.5 K and it forms an azeotrope with methanol at 336.9 K and 101.3 kPa[3]. It is nearly impossible to separate the azeotrope using the general distillation method to obtain the high-purity product but separation can be attained by special distillation method. In a previous experiment[4], methanol and dimethyl carbonate were separated by reactive and extractive distillation using phenol as a solvent. In the case of extractive distillation, an extra component was required as a solvent. On the contrary, the pressure-swing distillation (PSD) process[5], is an eco-friendly separation method that does not require a third component.

The pressure-swing distillation process is a useful method for separating the azeotrope because the azeotropic mole composition can be desirably varied based on the operating pressure. Fig. 2 shows the vapor-liquid equilibrium (VLE) diagram for the methanol-dimethyl carbonate system at low pressure and high pressure, respectively. The dotted line and solid line respectively represent the vapor-liquid equilibrium diagram at low pressure and high pressure.

In Fig. 3, the methanol-dimethyl carbonate binary mixture is first fed to the distillation column. The composition profile of methanol varies according to the dotted line because this column is operated at low pressure. High-purity methanol can be obtained at the bottom of this column and the approximate azeotropic composition can be obtained at the top. After

pressurizing using a pump, the top stream of the first column is fed to the second distillation column that operates at high pressure. At this point, the vapor-liquid equilibrium diagram for the methanol-dimethyl carbonate approaches the solid line. Therefore, the approximate azeotropic composition at high pressure is obtained at the top of this column. This stream is refluxed to the top of the first distillation column. High-purity dimethyl carbonate can be obtained at the bottom of the second distillation column.

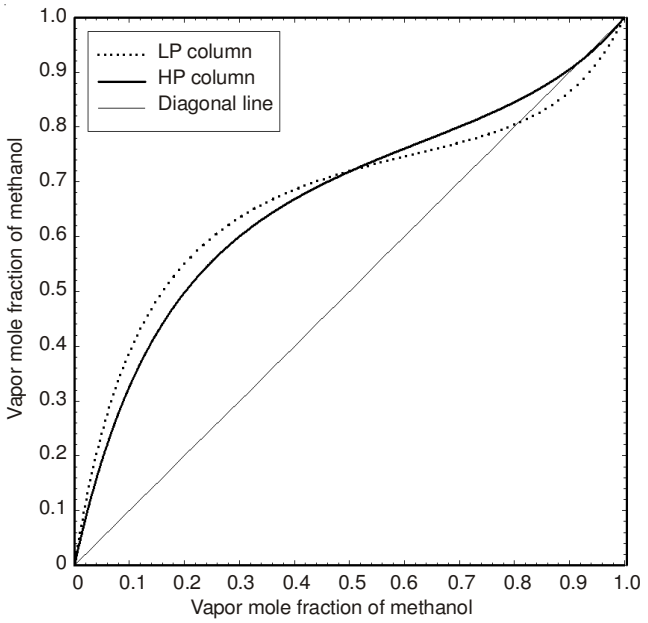

Fig. 2. Vapor-liquid equilibrium diagrams for methanol-dimethyl carbonate system at low-pressure and high-pressure

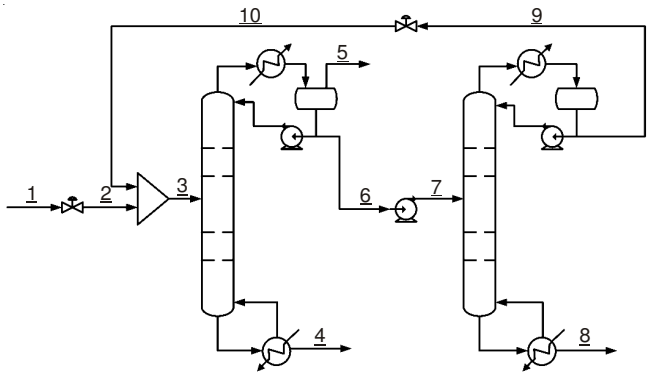

Fig. 3. Schematic diagram of pressure-swing distillation for low-high pressure column configuration

On the other hand, as shown in Fig. 4, high-purity dimethyl carbonate can be obtained at the bottom of the first distillation column. High-purity methanol can be obtained at the bottom of the second distillation column which is operated at low pressure.

In order to accurately simulate the design of the pressure-swing distillation process, it is important to select the correct thermodynamic model and binary interaction parameter (BIP). However, general chemical process simulators such as PRO/II, Aspen Plus and Chem CAD do not have a built-in binary interaction parameter for the methanol-dimethyl carbonate system. Therefore, in this study, the vapor-liquid equilibrium

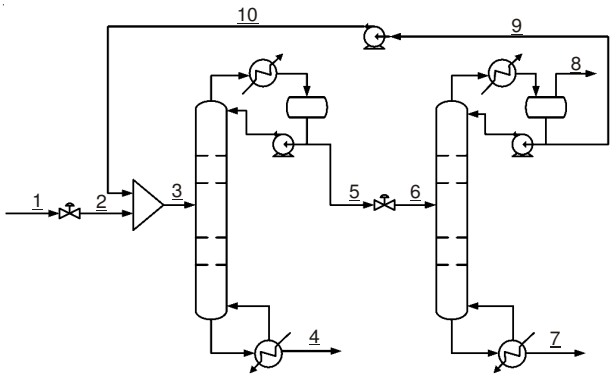

Fig. 4. Schematic diagram of pressure-swing distillation for high-low pressure column configuration

of the methanol-dimethyl carbonate binary system was experimentally evaluated and the binary interaction parameters were deduced from the non-random two-liquid (NRTL) model regression using the experimental data. The obtained binary interaction parameters were then applied to the pressure-swing distillation process modeling.

Simulations were performed with the objective of producing high-purity dimethyl carbonate (99.5 wt. %) using Invensys PRO/II with PROVISION[6]. This can be achieved either by using the high-low pressure column configuration or the low-high pressure column configuration. After performing the simulations, the total heat duties of the reboiler were compared.

THEORY

In order to simulate the pressure-swing distillation process, the non-random two-liquid activity coefficient model[7,8] is used to analyze the non-ideality between methanol and dimethyl carbonate for the liquid phase. The Soave-Redlich-Kwong (SRK) equation of state[9] is used to interpret the non-ideality under high-pressure conditions in the vapor phase. The non-random two-liquid model is expressed as eqn. (1).

$$\ln \gamma_i = \frac{\Sigma_i \tau_{ji} G_{ji} x_j}{\Sigma_k G_{ki} x_k} + \Sigma_j \frac{x_j G_{ij}}{\Sigma_k G_{kj} x_k}\left(\tau_{ij} - \frac{\Sigma_k x_k \tau_{kj} G_{kj}}{\Sigma_k G_{kj} x_k}\right) \quad (1)$$

where, τ_{ij} and G_{ij} in eqn. (1) can be expressed as eqns. (2), (3) and (4).

$$\tau_{ij} = a_{ij} + \frac{b_{ij}}{T} \quad (2)$$

$$G_{ij} = \exp(-a_{ij}\tau_{ij}) \quad (3)$$

$$a_{ij} = \alpha'_{ij} + \beta'_{ij} T \quad (4)$$

In eqns. (2) and (4), T indicates the absolute temperature. The non-random two-liquid liquid activity coefficient model in eqn. (1) has six binary interaction parameters. *i.e.*, a_{ij}, a_{ji}, b_{ij}, b_{ji}, α_{ij} and β_{ij}, including a temperature-dependent term for each binary system.

Eqn. (5) expresses the SRK equation of state applied to the vapor phase.

$$P = \frac{RT}{v-b} - \frac{a\alpha}{v(v+b)} \quad (5)$$

The parameters a and b in eqn. (5) can be expressed as eqns. (6) and (7), respectively, as a function of critical

temperature and critical pressure. The energy parameter, a, and size parameter, b, is shown below.

$$a_i = 0.42747\frac{R^2T_{ci}^2}{P_{ci}} \quad (6)$$

$$b_i = 0.08664\frac{RT_{ci}}{P_{ci}} \quad (7)$$

EXPERIMENTAL

Methanol (99.9 %, HPLC grade) and dimethyl carbonate (99.5 %, GR grade) were supplied by Samchun Pure Chemical Co. Ltd., Korea. Methanol and dimethyl carbonate were used without further purification.

Preparation of standard solutions: To determine the accurate concentration of the samples that were collected in the vapor-liquid equilibrium experiments, a standard curve must be constructed from standard solution with various concentrations of the methanol and dimethyl carbonate binary mixture. Thus, a total number of 11 standard solutions were subjected to gas chromatography (GC) analysis. The standard solutions comprised a total mass of 20 g and concentration was varied from 0 to 100 wt. % with an interval of 10 wt. % based on methanol. Table-1 shows the mass concentration of methanol in the actual mixture which was calculated by considering the purity and weight of the reagents.

Analysis: The compositions of the condensed vapor and liquid phases were analyzed using a YL6100 GC and a HT300A autosampler with an FID detector. A Carbowax capillary (30 m × 0.32 mm × 0.25 μm) was used as the chromatographic column. Helium was used as a carrier gas for the analysis. Fig. 5 shows the calibration curve for the methanol-dimethyl carbonate binary system.

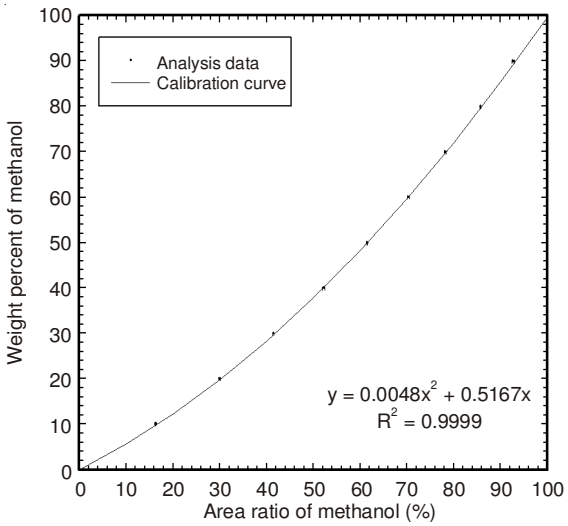

Fig. 5. Calibration curve for methanol-dimethyl carbonate system

Vapor-liquid equilibrium experiments: A Fischer vapor-liquid equilibrium 602 type apparatus was used for the vapor-liquid equilibrium experiment. The vapor-liquid equilibrium apparatus is shown in Fig. 6. The names of the parts of the vapor-liquid equilibrium experimental equipment are shown in Table-2. After filling the mixing chamber with methanol,

TABLE-1
CALCULATED MASS CONCENTRATION OF METHANOL IN THE ACTUAL MIXTURE

Concentration of MeOH (wt. %)	Weight of MeOH (g)	Weight of dimethyl carbonate (g)	Total weight (g)	Calculated weight of MeOH (g)	Calculated concentration of MeOH (wt. %)
0	0.00	20.00	20.00	0.000	0.00
10	2.01	17.99	20.00	2.008	10.04
20	4.00	15.99	19.99	3.996	19.99
30	6.00	14.00	20.00	5.994	29.97
40	8.00	12.00	20.00	7.992	39.96
50	10.00	10.00	20.00	9.990	49.95
60	12.01	7.99	20.00	11.998	59.99
70	14.00	6.01	20.01	13.986	69.70
80	16.00	4.00	20.00	15.984	79.92
90	18.00	2.00	20.00	17.982	89.91
100	20.00	0.00	20.00	19.980	99.90

TABLE-2
NAMES OF PARTS ON VAPOUR-LIQUID EQUILIBRIUM EXPERIMENTAL EQUIPMENT

No.	Name	No.	Name
1	Heater	14	Solenoid: condensed vapor sample
2	Cottrell-pump	15	Receiver: liquid sample
3	Separation chamber	16	Receiver: vapor sample
4	Condenser	17	Valve: pressure equilibrium to sample tube no. 15
5	Security cooler vapor phase	18	Valve: pressure equilibrium to sample tube no. 16
6	Security cooler liquid phase	19	Ventilation valve liquid phase
7	Mixing chamber with PTFE stirrer bar	20	Ventilation valve vapor phase
8	Pt-100: vapor temperature	21	Valve: liquid sample
9	Pt-100: liquid temperature in the evaporator	22	Valve: vapor sample
10	Septum: liquid sample	23	Discharge valve
11	Septum: condensed vapor sample	24	Pt-100: temperature control of heated tube
12	Septum: vapor sample	25	Pt-100: temperature control of heated isolation jacket
13	Solenoid: liquid sample	26	Connection to buffer vessel

the control box was used to maintain a constant pressure. The constant low pressure (30 kPa) was maintained using a vacuum pump and constant atmospheric pressure (101.3 kPa) was maintained using nitrogen gas. Methanol was boiled by increasing the temperature of the liquid phase using a heater. The temperature of the vapor phase also increased because methanol vapor was generated. State of equilibrium was reached and maintained at constant pressure and temperature. At the same time, the temperature was recorded. Samples of the condensed vapor and liquid phase were collected. After adding dimethyl carbonate using a pipette, the process was repeated for 20 times using the same method. The collected samples were quantitatively analyzed using gas chromatography.

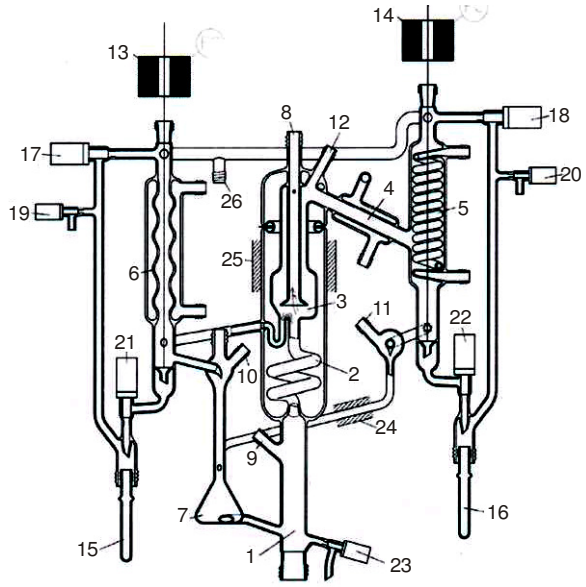

Fig. 6. Apparatus for vapor-liquid equilibrium experiment

RESULTS AND DISCUSSION

Vapor-liquid equilibrium experiments: Isobaric vapor-liquid equilibrium data for the methanol-dimethyl carbonate binary system was acquired at low pressure (30 kPa) and atmospheric pressure (101.3 kPa). The experimental vapor-liquid equilibrium data and results are listed in Tables 3 and 4. The experimental vapor-liquid equilibrium data in the form of Txy and xy plots are shown in Figs. 7-10.

Results of regression: The NRTL-RK model was used to correlate the vapor-liquid equilibrium data for the binary system at different pressures. In order to fit the binary interaction parameters, the maximum technical term equation [Eqn. (8)] was used as the following objective function. In the maximum technical term objective function, errors of all variables such as T, P, x and y are considered[10].

$$F = \Sigma_{n=1}^{NDG} w_n \Sigma_{i=1}^{NP} \left[\left(\frac{T_{e,i} - T_{m,i}}{T_{m,i}} \right)^2 + \left(\frac{P_{e,i} - P_{m,i}}{P_{m,i}} \right)^2 + \Sigma_{j=1}^{NC-1} \left(\frac{x_{e,i,j} - x_{m,i,j}}{x_{m,i,j}} \right)^2 + \Sigma_{j=i}^{NC-1} \left(\frac{y_{e,i,j} - y_{m,i,j}}{y_{m,i,j}} \right)^2 \right] \quad (8)$$

TABLE-3
EXPERIMENTAL VAPOUR-LIQUID EQUILIBRIUM DATA FOR METHANOL(1) AND DIMETHYL CARBONATE (2) AT 30 kPa

Temperature (K)	x_1	y_1
309.69	1.0000	1.0000
309.49	0.9879	0.9791
309.28	0.9772	0.9624
309.11	0.9670	0.9476
308.87	0.9515	0.9264
308.69	0.9369	0.9090
308.44	0.9034	0.8715
308.36	0.8772	0.8495
308.27	0.8122	0.8097
308.32	0.7751	0.7938
308.36	0.7449	0.7836
308.40	0.7196	0.7760
308.48	0.6922	0.7671
308.68	0.6365	0.7506
309.40	0.4951	0.7073
310.06	0.3966	0.6784
311.91	0.2681	0.6222
314.90	0.1628	0.5223
318.34	0.0970	0.3963
322.43	0.0540	0.2573
324.83	0.0349	0.1671
329.40	0.0000	0.0000

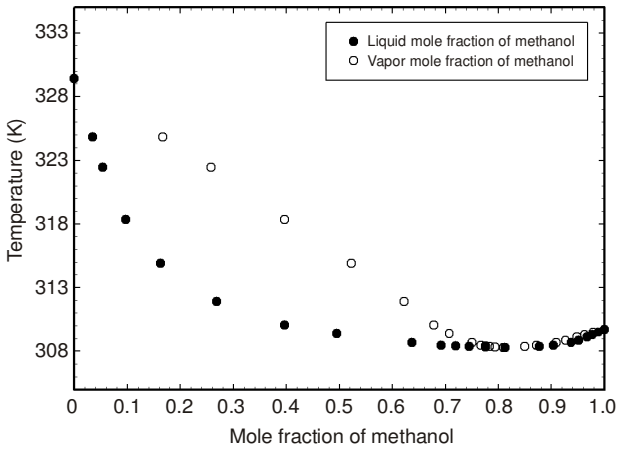

Fig. 7. Txy plot for experimental vapor-liquid equilibrium (VLE) data at 30 kPa

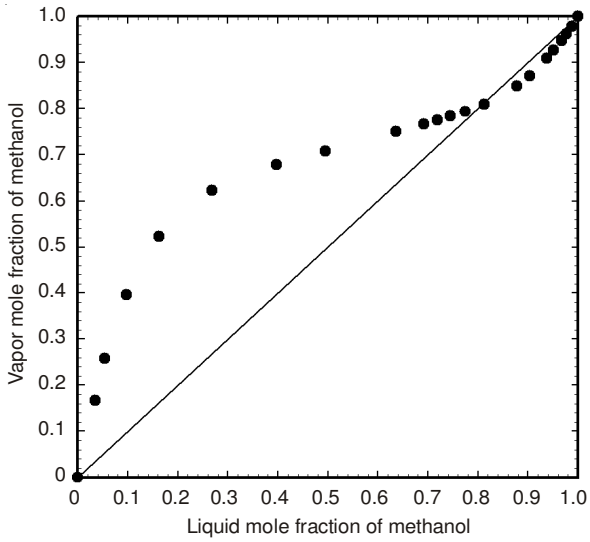

Fig. 8. xy plot for experimental vapor-liquid equilibrium (VLE) data at 30 kPa

TABLE-4
EXPERIMENTAL VAPOUR-LIQUID EQUILIBRIUM DATA FOR METHANOL (1) AND DIMETHYL CARBONATE (2) AT 101.3 kPa

Temperature (K)	x_1	y_1
337.71	1.0000	1.0000
337.46	0.9838	0.9755
337.36	0.9755	0.9636
337.11	0.9530	0.9332
337.02	0.9405	0.9211
336.98	0.9324	0.9136
336.87	0.9106	0.8930
336.82	0.8923	0.8785
336.78	0.8768	0.8685
336.77	0.8647	0.8593
336.78	0.8449	0.8497
336.79	0.8276	0.8399
336.80	0.8177	0.8345
336.83	0.7970	0.8252
337.00	0.7403	0.8051
337.32	0.6657	0.7831
338.38	0.5139	0.7451
339.35	0.4262	0.7178
341.51	0.3120	0.6677
343.36	0.2434	0.6202
347.47	0.1575	0.5147
351.59	0.1018	0.3918
355.89	0.0627	0.2619
359.31	0.0356	0.1492
363.26	0.0000	0.0000

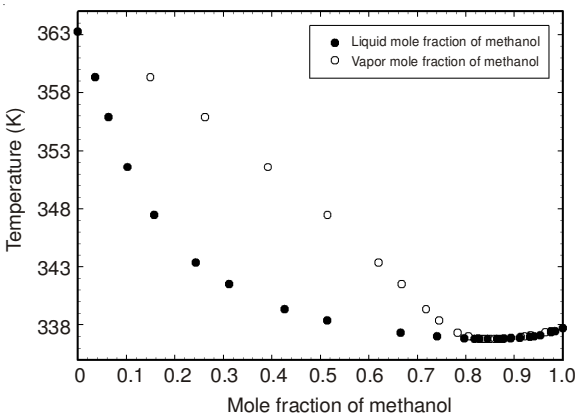

Fig. 9. Txy plot for experimental vapor-liquid equilibrium (VLE) data at 101.3 kPa

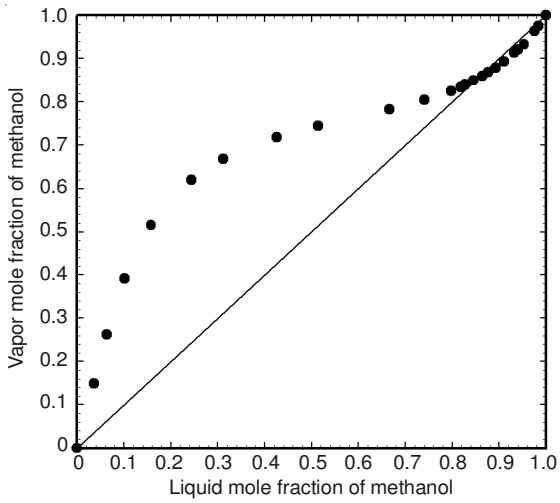

Fig. 10. xy plot for experimental vapor-liquid equilibrium (VLE) data at 101.3 kPa

The xy plots of the results of the NRTL regression are shown in Figs. 11 and 12. The result in Fig. 13 shows the isobaric vapor-liquid equilibrium data acquired by Wang *et al.*[4] at 1013 kPa used for the regression analysis, since the vapor-liquid equilibrium experiments were not performed under high-pressure conditions.

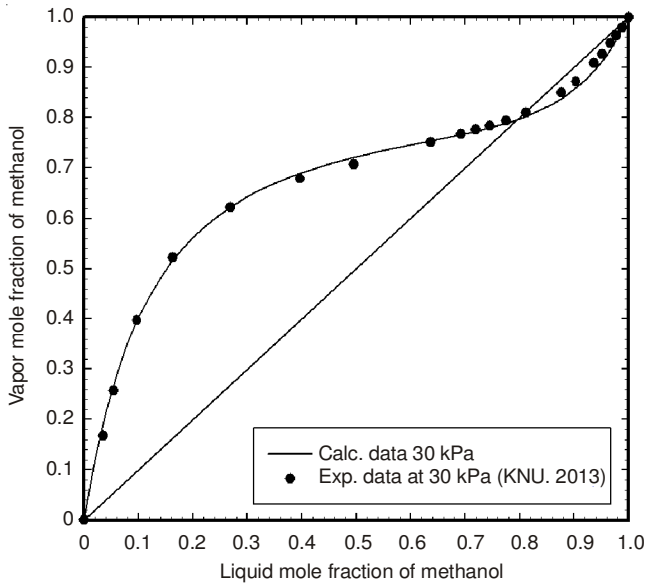

Fig. 11. Comparison between experimental vapor-liquid equilibrium (VLE) data and calculated data by NRTL regression analysis at 30 kPa

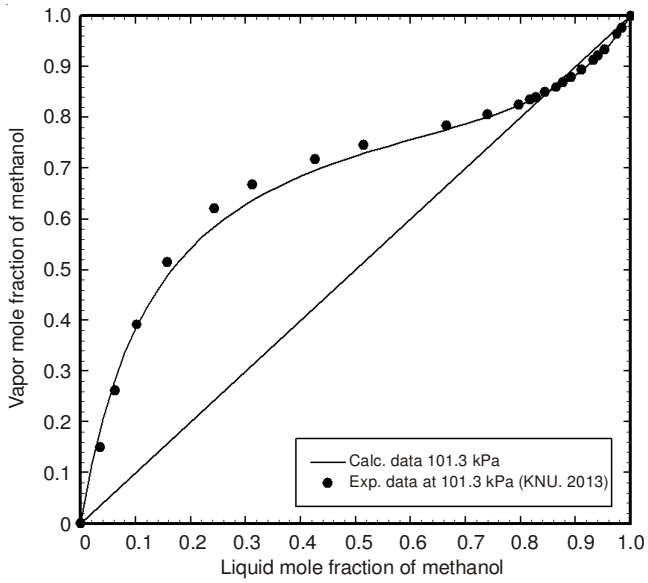

Fig. 12. Comparison between experimental vapor-liquid equilibrium (VLE) data and calculated data by NRTL regression analysis at 101.3 kPa

The parameters for the NRTL-RK model regression under low, atmospheric and high-pressure conditions are listed in Table-5. Comparison of the experimental and calculated data for the azeotropic point and molar composition of methanol are listed in Table-6.

The average absolute deviations (AAD) % for the vapor phase mole fractions of methanol were obtained using the experimental results and the calculated data. The AAD (%)

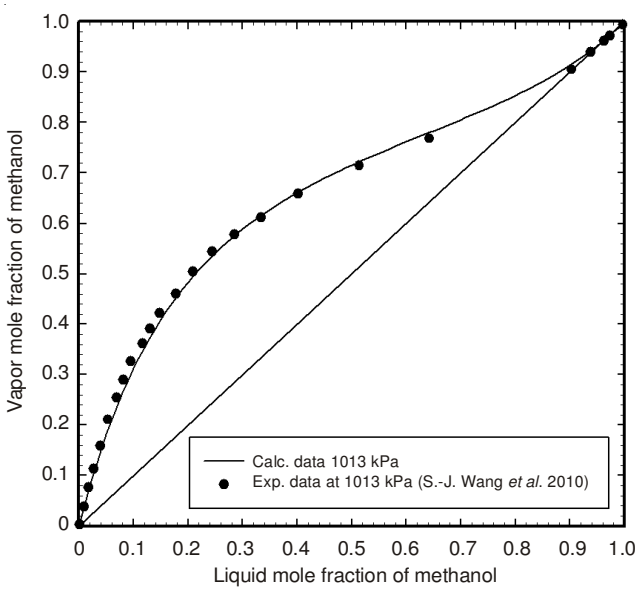

Fig. 13. Comparison between experimental vapor-liquid equilibrium (VLE) data and calculated data by NRTL regression analysis at 1013 kPa

TABLE-5
NRTL-RK BINARY INTERACTION PARAMETERS
FOR METHANOL (1)-DIMETHYL CARBONATE (2) SYSTEM

Pressure (kPa)	a_{12} a_{21}	b_{12} b_{21}	α_{12}	β_{12}
30	-11.844 4.9493	4155.7 -1502.7	0.3	-0.000229
101.3	-7.6996 4.4904	3026.1 -1464.2	0.3	-
1013	1.9009 -1.9085	-392.89 784.54	0.3	-

can be defined using eqn. (9) and the results are shown in Table-7.

$$AAD\ (\%) = \left(\frac{100}{N}\right)\Sigma_j^N \left|y_j^{exp} - y_j^{cal}\right| \quad (9)$$

Design and optimization of pressure-swing distillation process: To facilitate the comparison of the energy consumption of the pressure-swing distillation process for refining dimethyl carbonate to 99.5 wt. % using the high-low pressure column configuration and the low-high pressure column configuration, feedstock information was obtained from a research paper by Wei *et al.*[11]. Table-8 shows feedstock information for the mole composition, temperature, pressure and flow rates. The purity of methanol and dimethyl carbonate at the bottom of the distillation column was 99.5 wt. %. The methanol composition at the top of the distillation column was improved to start the optimization process. Subsequently, the number of theoretical stages was determined based on the various reflux ratios. The optimal point was determined from the graph of the number of theoretical stages and the reflux ratio. Finally, the optimal feed tray location was determined based on the minimum total reboiler heat duty.

TABLE-7
RESULTS OF AVERAGE ABSOLUTE
DEVIATION (%) CALCULATION

Pressure (kPa)	Average absolute deviation (%)
30	0.8530
101.3	0.9809
1013	0.7039

TABLE-8
FEEDSTOCK INFORMATION

Component	Value
Methanol	95.64
Dimethyl carbonate	4.16
Ammonia	0.20
Total flow (kmol/h)	10.98
Temperature (K)	318.15
Pressure (kPa)	202.65

Design and optimization of high-low pressure column configuration: The reboiler heat duty of the high-pressure and low-pressure columns based on various mole percentages of methanol ranging from 93.6 to 94.4 mol % in the high-pressure column (T01) is shown in Fig. 14. The minimum total reboiler heat duty of the high-pressure and low-pressure columns was 0.9698×10^6 kcal/h with a composition of 93.6 mol % methanol in the high-pressure column (T01), as shown in Fig. 15. The reboiler heat duty of the high-pressure and low-pressure columns based on various mole percentages of methanol ranging from 85 to 87 mol % in the low-pressure column (T02) are shown in Fig. 16. The minimum total reboiler heat duty of the high-pressure and low-pressure columns was 0.9698×10^6 kcal/h with a composition of 86.0 mol % methanol in the low-pressure column (T02), as shown in Fig. 17.

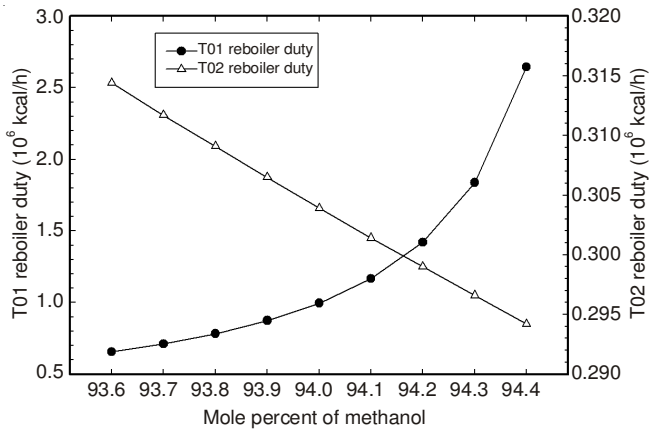

Fig. 14. Reboiler heat duty of high-pressure and low-pressure columns based on various mole percentages of methanol in high-pressure column (T01)

TABLE-6
COMPARISON OF EXPERIMENTAL DATA AND CALCULATED DATA
FOR AZEOTROPIC POINT AND MOLAR COMPOSITION OF METHANOL

Pressure (kPa)	Azeotropic molar composition		Azeotoropic point (K)	
	Exp.	Calc.	Exp.	Calc.
30	0.81	0.7969	308.28	307.86
101.3	0.85	0.8599	336.77	336.60
1013	0.9621	0.9610	410.24	410.33

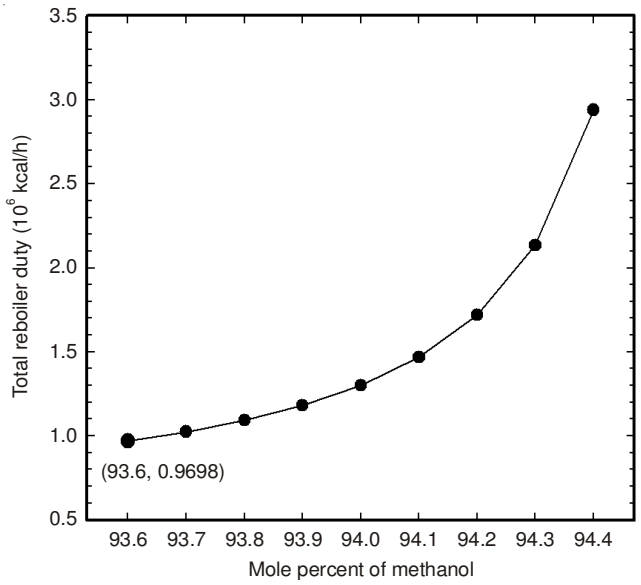

Fig. 15. Total reboiler heat duty of high-pressure and low-pressure columns based on various mole percentages of methanol in high-pressure column (T01)

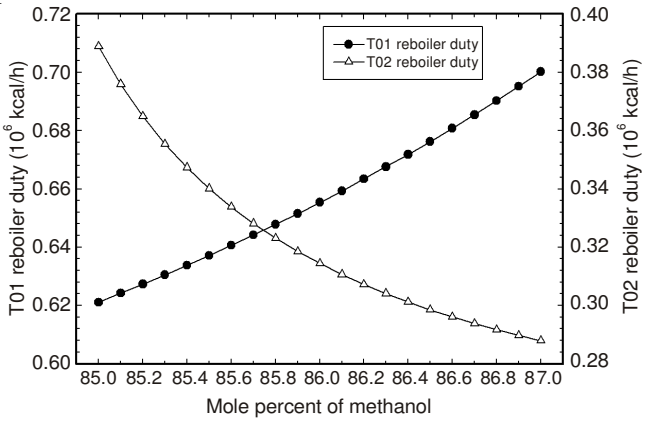

Fig. 16. Reboiler heat duty of high-pressure and low-pressure columns based on various mole percentages of methanol in low-pressure column (T02)

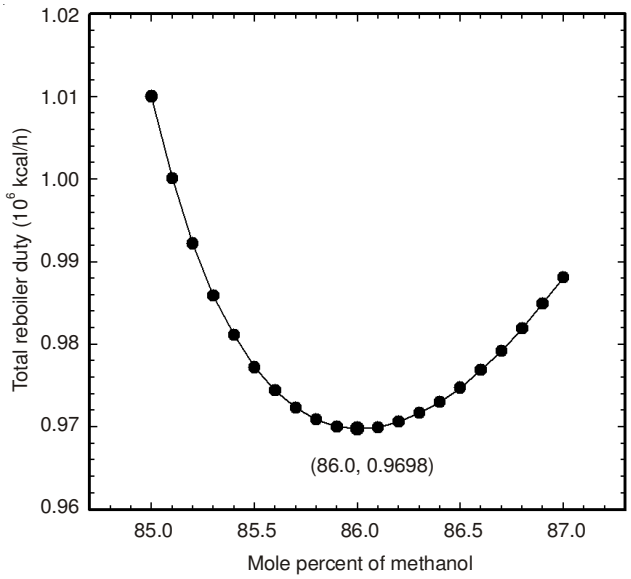

Fig. 17. Total reboiler heat duty of high-pressure and low-pressure columns based on various mole percentages of methanol in low-pressure column (T02)

The graph of the number of theoretical stages based on the various reflux ratios at T01 and T02 are shown in Figs. 18 and 19. The number of theoretical stages is inversely proportional to the reflux ratio; the higher the reflux ratio, the fewer the number of theoretical stages. However, the operational cost would be high because the heat duty of the condenser and reboiler is increased. On the other hand, decreasing the reflux ratio would lower the operational cost. However, the initial investment cost would increase owing to the rapid increase in the number of theoretical stages.

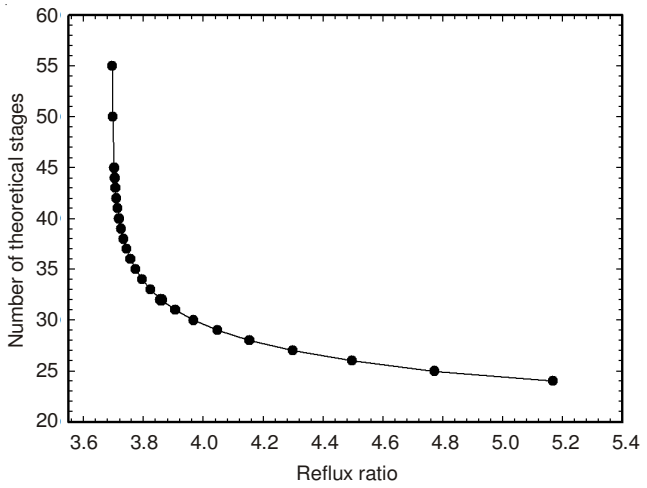

Fig. 18. Number of theoretical stages based on various reflux ratios at high-pressure column (T01)

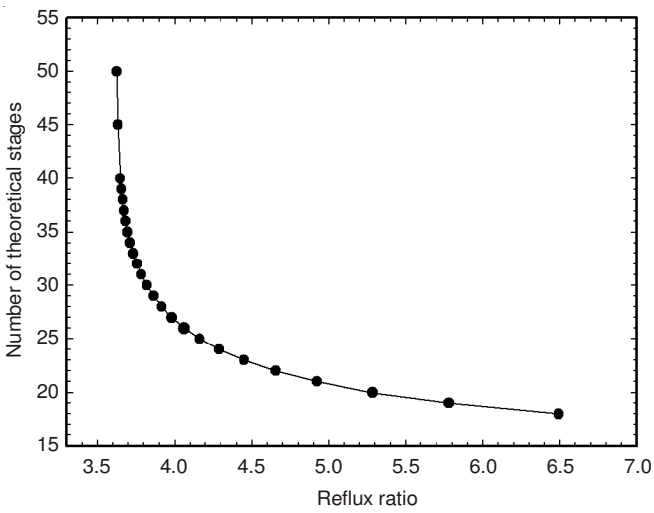

Fig. 19. Number of theoretical stages based on various reflux ratios at low-pressure column (T02)

Therefore, the minimum total operational cost and the initial investment cost must be determined[12]. The number of theoretical stages was 32 and 26 for T01 and T02, respectively.

The graphs of the reboiler heat duties based on various feed tray locations for the two columns are shown in Figs. 20 and 21. The optimum feed tray locations were at the 16th stage for T01 and at the 9th stage for T02. Thus, the minimum total reboiler heat duty was 0.8991×10^6 kcal/h.

The results of analysis of the heat and material balance of the pressure-swing distillation process for the high-low pressure column configuration are listed in Tables 9 and 10.

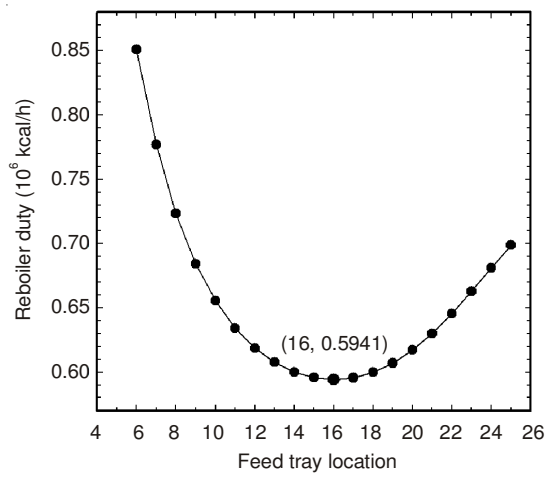

Fig. 20. Reboiler heat duty based on various feed tray locations for high-pressure column (T01)

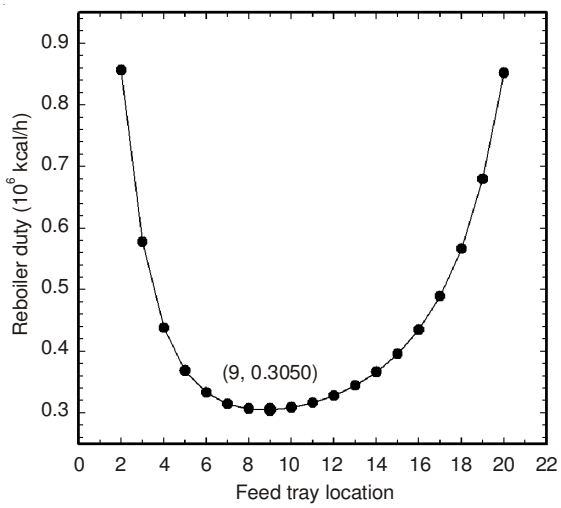

Fig. 21. Reboiler heat duty based on various feed tray locations for low-pressure column (T02)

These results were compared with the results (1.0510×10^6 kcal/h) published by Wei *et al.*[11]. A suitable fit was achieved through the NRTL model regression using the obtained binary interaction parameters.

Design and optimization of low-high pressure column configuration: The method used for the high-low pressure column configuration can be applied for optimization of the low-high pressure column configuration. The reboiler heat duties of the high-pressure and low-pressure columns based on various mole percentages of methanol in the low-pressure column (T01) are shown in Figs. 22 and 23. From this data, the optimum methanol composition is 85.6 mol % at T01. The minimum total reboiler heat duty was indicated to be 0.4373×10^6 kcal/h when the mole percentage of methanol is 91.4 mol % in the high-pressure column (T02). The results are shown in Figs. 24 and 25.

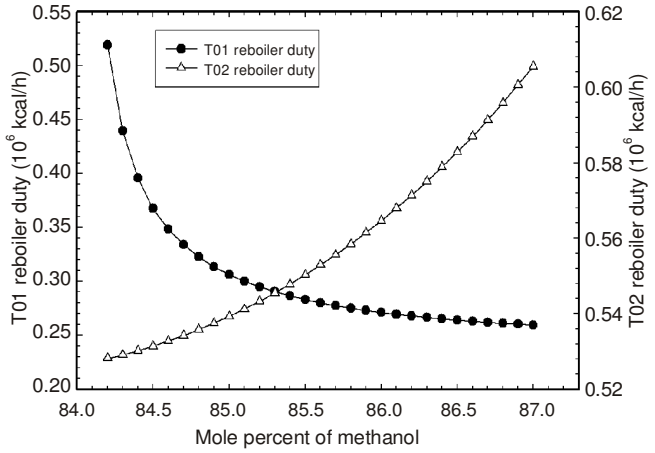

Fig. 22. Reboiler heat duty of low-pressure and high-pressure columns based on various mole percentages of methanol in low-pressure column (T01)

TABLE-9
HEAT AND MATERIAL BALANCE ANALYSIS OF PRESSURE-SWING DISTILLATION PROCESS FOR HIGH-LOW PRESSURE COLUMN CONFIGURATION (1)

Stream name	1		2		3		4		5	
Temperature (K)	318.15		318.15		325.61		464.47		414.02	
Pressure (kPa)	202.65		1215.90		1215.90		1229.42		1200.00	
Flow rate (kmol/h)	10.98		10.98		18.92		0.41		18.51	
Flow rate (kg/h)	378.00		378.00		690.16		36.80		653.37	
	mol %	wt %	mol %	wt %	mol %	wt %	mol %	wt %	mol %	wt %
Methanol	95.64	89.01	95.64	89.01	91.59	80.46	1.39	0.50	93.60	84.97
Dimethyl carbonate	4.16	10.89	4.16	10.89	7.80	19.25	98.61	99.50	5.77	14.73
Ammonia	0.20	0.10	0.20	0.10	0.61	0.29	0.00	0.00	0.63	0.30

TABLE-10
HEAT AND MATERIAL BALANCE ANALYSIS OF PRESSURE-SWING DISTILLATION PROCESS FOR HIGH-LOW PRESSURE COLUMN CONFIGURATION (2)

Stream name	6		7		8		9		10	
Temperature (K)	347.48		342.72		334.15		334.15		334.98	
Pressure (kPa)	151.99		123.54		100.00		100.00		1300.00	
Flow rate (kmol/h)	18.51		10.32		0.25		7.94		7.94	
Flow rate (kg/h)	653.37		331.64		9.66		312.13		312.13	
	mol %	wt %	mol %	wt %	mol %	wt %	mol %	wt %	mol %	wt %
Methanol	93.60	84.97	99.82	99.50	78.48	65.96	86.00	70.11	86.00	70.11
Dimethyl carbonate	5.77	14.73	0.18	0.50	12.75	30.12	12.82	29.38	12.82	29.38
Ammonia	0.63	0.30	0.00	0.00	8.77	3.92	1.18	0.51	1.18	0.51

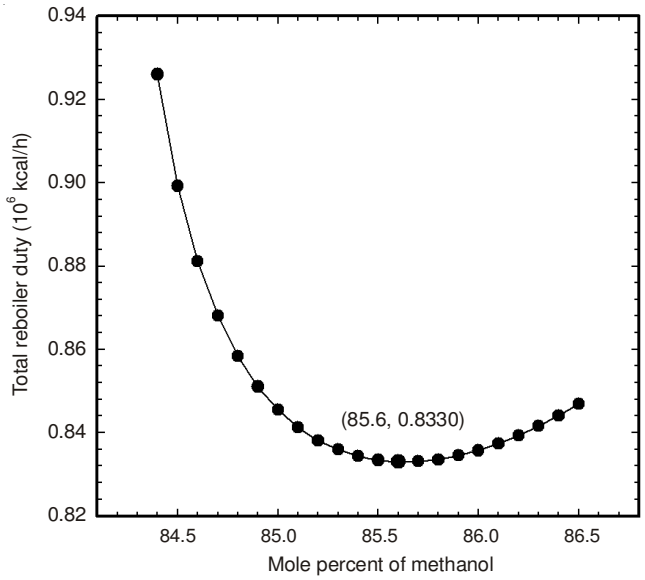

Fig. 23. Total reboiler heat duty of low-pressure and high-pressure columns based on various mole percentages of methanol in low-pressure column (T01)

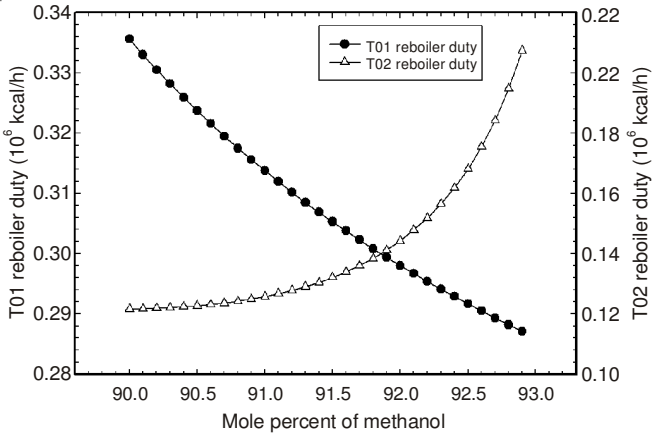

Fig. 24. Reboiler heat duty of low-pressure and high-pressure columns based on various mole percentages of methanol in high-pressure column (T02)

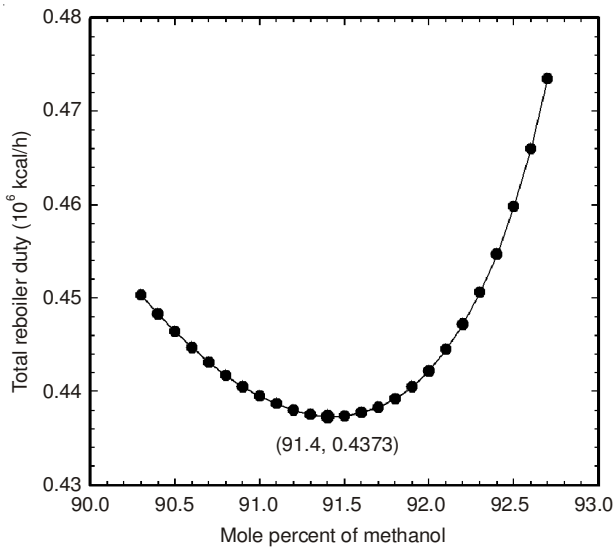

Fig. 25. Total reboiler heat duty of low-pressure and high-pressure columns based on various mole percentages of methanol in high-pressure column (T02)

The graphs of the number of theoretical stages based on various reflux ratios are shown in Figs. 26 and 27. The number of theoretical stages were 28 for T01 and 25 for T02.

The graphs of the optimum feed tray location for the two columns are shown in Figs. 28 and 29. The optimum feed tray locations are at the 10th stage for T01 and at the 15th stage for T02. Therefore, the minimum total reboiler heat duty is 0.4279×10^6 kcal/h. An energy reduction effect of 52.4 % is achieved with the low-high pressure column configuration compared to the conventional high-low pressure column configuration.

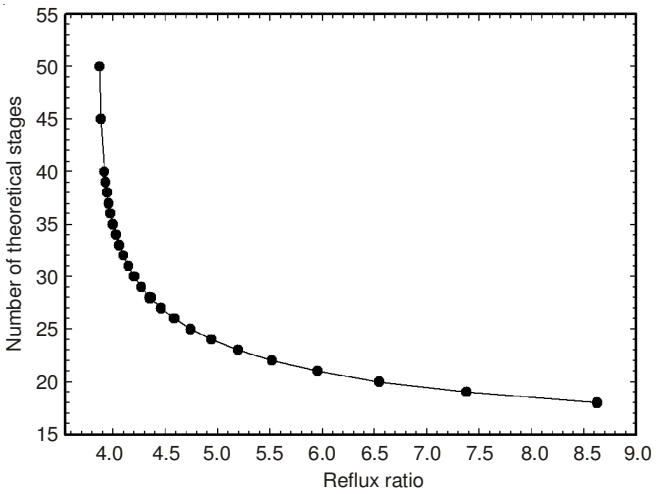

Fig. 26. Number of theoretical stages based on various reflux ratios at low-pressure column (T01)

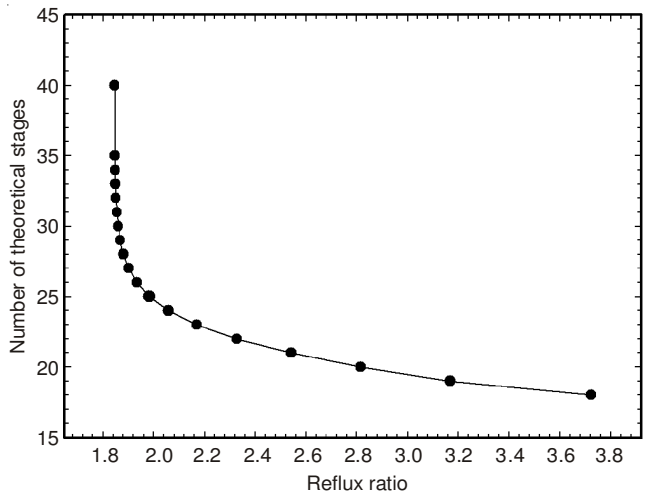

Fig. 27. Number of theoretical stages based on various reflux ratios at high-pressure column (T02)

The results of the heat and material balance analysis of the pressure-swing distillation process for the low-high pressure column configuration are presented in Tables 11 and 12.

Application of heat integration: Herein, the heat integration process[5] is suggested as a means of reducing the reboiler heat duties in the pressure-swing distillation process. As shown in Fig. 30, the heat integration process can be utilized for the combination of respective streams when the removed heat duty of the condenser is equal to the applied heat duty of the reboiler.

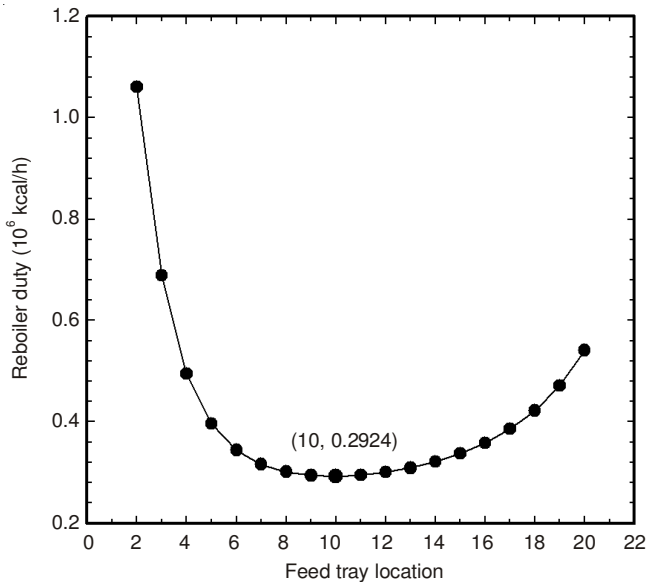

Fig. 28. Reboiler heat duty based on various feed tray locations for low-pressure column (T01)

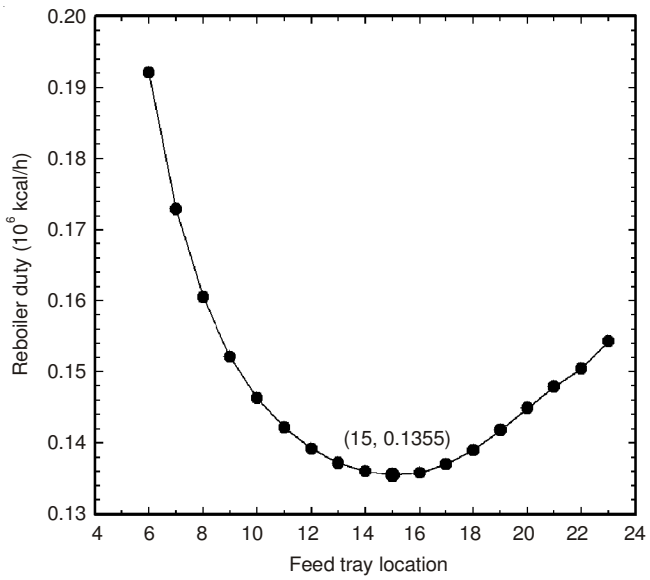

Fig. 29. Reboiler heat duty based on various feed tray locations for high-pressure column (T02)

In this process, the removed heat duty of the condenser at the high-pressure column is 0.1217 × 10^6 kcal/h and the applied heat duty of the reboiler at the low-pressure column is 0.2924 × 10^6 kcal/h. The substantive heat duty can be reduced to 0.1707 × 10^6 kcal/h owing to the effect of heat integration. Therefore, when heat integration is applied, the total reboiler heat duty can be reduced to 0.3062 × 10^6 kcal/h. The energy reduction effect of the low-high pressure column configuration with heat integration resulted in a 65.9 % decrease in heat duty compared with the conventional high-low pressure column configuration.

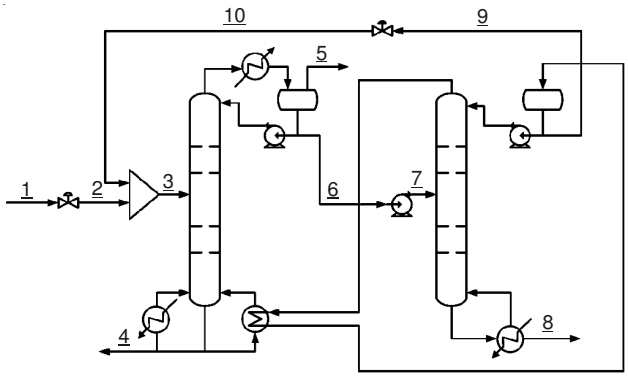

Fig. 30. Schematic diagram of pressure-swing distillation for low-high pressure configuration with heat integration

TABLE-11
HEAT AND MATERIAL BALANCE ANALYSIS OF PRESSURE-SWING DISTILLATION PROCESS FOR LOW-HIGH PRESSURE COLUMN CONFIGURATION (1)

Stream name	1		2		3		4		5	
Temperature (K)	318.15		318.15		345.66		343.14		334.15	
Pressure (kPa)	202.65		151.99		151.99		125.50		100.00	
Flow rate (kmol/h)	10.98		10.98		16.96		10.32		0.25	
Flow rate (kg/h)	378.00		378.00		593.81		331.63		9.72	
	mol %	wt %	mol %	wt %	mol %	wt %	mol %	wt %	mol %	wt %
Methanol	95.64	89.01	95.64	89.01	94.14	86.13	99.82	99.50	78.26	65.54
Dimethyl carbonate	4.16	10.89	4.16	10.89	5.28	13.59	0.18	0.50	12.98	30.57
Ammonia	0.20	0.10	0.20	0.10	0.58	0.28	0.00	0.00	8.75	3.90

TABLE-12
HEAT AND MATERIAL BALANCE ANALYSIS OF PRESSURE-SWING DISTILLATION PROCESS FOR LOW-HIGH PRESSURE COLUMN CONFIGURATION (2)

Stream name	6		7		8		9		10	
Temperature (K)	334.15		334.98		464.17		411.18		346.93	
Pressure (kPa)	100.00		1300.00		1222.56		1200.00		151.99	
Flow rate (kmol/h)	6.39		6.39		0.41		5.97		5.97	
Flow rate (kg/h)	252.49		252.49		36.74		215.77		215.77	
	mol %	wt %	mol %	wt %	mol %	wt %	mol %	wt %	mol %	wt %
Methanol	85.60	69.37	85.60	69.37	1.39	0.50	91.40	81.10	91.40	81.10
Dimethyl carbonate	13.22	30.12	13.22	30.12	98.61	99.50	7.34	18.31	7.34	18.31
Ammonia	1.18	0.51	1.18	0.51	0.00	0.00	1.26	0.59	1.26	0.59

Conclusion

The vapor-liquid equilibrium for the methanol-dimethyl carbonate binary system was experimentally evaluated herein. The binary interaction parameters in the non-random two-liquid model were deduced using the experimental vapor-liquid equilibrium data. The modified non-random two-liquid model was applied to the pressure-swing distillation process for producing 99.5 wt. % dimethyl carbonate using Invensys PRO/II with PROVISION. In order to minimize the energy consumption of the process, the optimal methanol composition was determined along with the optimum number of theoretical stages and the feed tray location for the two columns. The low-high pressure column configuration was superior because the energy consumption of this configuration was less than that of the conventional high-low pressure column configuration. The heat duties could be reduced to 65.9 % by application of heat integration in the process.

ACKNOWLEDGEMENTS

This research was supported by a grant from LNG Plant R&D Center founded by Ministry of Land, Transportation and Maritime affairs (MLTM) of the Korean government.

REFERENCES

1. H. Niu, H. Guo, J. Yao, Y. Wang and G. Wang, *J. Mol. Catal. A Chem*., **259**, 292 (2006).
2. E.-S. Jeong, K.-H. Kim, D.-W. Park and S.-W. Park, *Applied Chem*., **8**, 593 (2004).
3. A. Rodriguez, J. Canosa, A. Dominguez and J. Tojo, *Fluid Phase Equilib*., **201**, 187 (2002).
4. S.-J. Wang, C.-C. Yu and H.-P. Huang, *Comput. Chem. Eng*., **34**, 361 (2010).
5. L.L. William and L.I. Chien, Design and Control of Distillation Systems for Separating Azeotropes, John Wiley & Sons, Inc (2010).
6. PRO/IITM Keyword Manual, Invensys Systems, Inc (2010).
7. H. Renon and J.M. Prausnitz, *Ind. Eng. Chem. Process Des. Dev*., **8**, 413 (1969).
8. H. Renon and J.M. Prausnitz, *AIChE J*., **14**, 135 (1968).
9. G. Soave, *Chem. Eng. Sci*., **27**, 1197 (1972).
10. J.A. Barker, *Aust. J. Chem*., **6**, 207 (1953).
11. H.-M. Wei, F. Wang, J.-L. Zhang, B. Liao, N. Zhao, F.-K. Xiao, W. Wei and Y.-H. Sun, *Ind. Eng. Chem. Res*., **52**, 11463 (2013).
12. PRO/II Application Briefs, Simulation Sciences Inc. (2005).